

# Binding free energy calculation and structural analysis for antigen-antibody complex

Yuichiro Takamatsu, Ayumu Sugiyama, Acep Purqon, Hidemi Nagao,  
and Kiyoshi Nishikawa

*Division of Mathematical and Physical Science, Graduate School of Natural Science and Technology,  
Kanazawa University, Kakuma, Kanazawa 920-1192, JAPAN*

**Abstract.** Recently, much attention has been directed to calculational prediction for binding free energy and structural analysis for biomolecule complex in solvate state. We investigated Influenza Hemagglutinin (wild type HA), mutated HA and its neutralize antibody Fab fragment complex in explicit solvent water molecules by molecular dynamics simulation(MD). B-factor and binding free energy of loop structures in the complex structure are calculated. The calculation result supports the experimental result in a qualitative tendency. MD calculation also shows that hydrogen bond distance differs between wild type HA and mutated HA, which contributes to the difference of binding free energy and structural stability. These result suggests that pattern of making hydrogen bonds in crystal structure are almost kept even in solvate state.

**Keywords:** Antigen-Antibody Complex, Molecular Dynamics, B-factor, Binding free energy, MM-PBSA

**PACS:** 87.15.By, 87.15.Kg

## INTRODUCTION

The human immunity mainly has two different systems from outer harmful microorganism, i.e., innate and adaptive immunities. Various biomacromolecules contribute to immune system. In particular, antibodies have a principle role in adaptive immunity. The functions and structures of antibody are well known[1]. As a rule, they bind specifically to molecules on pathogens(antigens) by molecular recognition. An important mechanism of antibody to recognize antigen depends on loop structures in complementarity determining regions (CDRs) in variable regions on Fab fragment. The CDRs are classified into two groups, i.e., one belongs to Heavy chain(VH):nearly 28-35, 49-59, 92-103, the other belongs to Light chain(VL):nearly 30-36, 49-65, 95-103 amino acids sequence, respectively. Some reversible non-bond binding forces between various amino acids contribute to the antigen-antibody interaction. Therefore, amino acids sequence pattern on the loop structures in CDRs are an important factor for molecular recognition to their high favorable antigen.

These antibody's structure has been studied by some devices, but it leaves nothing to be argued the computer simulation has much contribution to elucidation its detailed mechanism. Moreover, automated docking simulation of ligands[2], and computer based drug design[3] have been made a significant trend in the field of pharmaceutical chemistry. Some of these simulation is based on binding free energy calculation and structural analysis.

Practical approaches to calculate binding free energies are developed by many groups[4]. Recently it suggests

MM-PBSA[5], which method can be applied to a wide range of macromolecules and molecule complexes. L. T. Chong et al.[6], B. Kuhn et al.[7], and H. Gohlke et al.[8] applied MM-PBSA method to binding free energy calculation of biomolecules, and they obtained results with a good correlation to experiment. The investigation for calculation of absolute binding free energy could make possible to more concisely predict docking mechanism between ligand and receptor, and yield profit for pharmaceutical chemistry.

Furthermore, genetic engineering by site-directed mutagenesis could further tailor an antibody's binding sequences to its complementary epitope. It suggests the possibility to design antibody drug more efficiently if antibody engineering is collaborated with computer simulation to predict concise antigen-antibody binding free energy.

In this paper, we investigated Influenza Hemagglutinin (HA:strain H3N2), mutated HA, and its neutralize antibody Fab fragment complex, which binding disassociation constant was already investigated by previous study[9].

According to the experimental result of the crystal structure differences between wild type HA and mutated HA[9], the mutation causes structural distortion, and carbonyl oxygen of residue K156 is completely buried. It results in the loss of hydrogen bonding, and mutated HA affinity to antibody became 4000-fold lower than wild type HA's.

To dynamically verify the above static result, we carried out molecular dynamics simulation in explicit solvent water molecules, and calculated root-mean-square

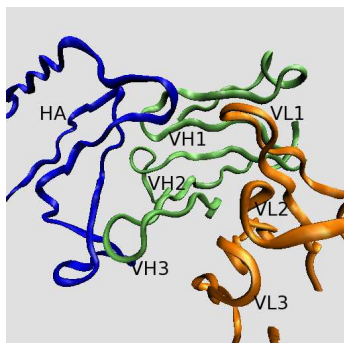


**FIGURE 1.** HA and CDRs loop structure in binding site.

deviations (RMSD) and fluctuations(B-factor) of loop structures of CDRs on Fab fragments in wild type HA. We made comparison the results of HA with those of mutated HA. The B-factor values correspond to structure stability of binding site[10]. At the same time, we calculated binding free energy of the complexes in crystal structure. After that, we compared the calculation results with disassociation constants which is derived from the experiment[9] above.

Finally, we kept track of distance between carboxyl oxygen on 156th lysine in HA and atoms on 131th threonine which are related to hydrogen bonding. We investigated the bond distance during molecular dynamics, and compared the result to that of mutated HA.

## METHOD

### Preparation

The initial atomic coordinates were extracted from crystal structures of the wild type HA(2VIR), and mutated HA(2VIS) in Protein Data Bank, respectively. The crystal structure shows that six loops of the CDRs in Fab fragments are packed and binds to HA(Fig. 1). We added hydrogen atom to crystal structures with the LEAP module of AMBER 8 program package[11]. Histidines in complex were protonated at the  $\delta$ -nitrogen. Amber03 force field parameter were adapted. We put TIP3P [12] water molecules 8.0 angstrom inside around complex molecules(Fig. 2), and neutralize the systems by counter ions.(Na<sup>+</sup> 2VIR, two Cl<sup>-</sup> 2VIS, respectively).

### Simulation

MD simulation was carried out by sander module in AMBER 8 program package. Non-bond long range interactions were cut off by 10.0 Angstroms. SHAKE algorithm was applied to 2VIS calculation, not to 2VIR

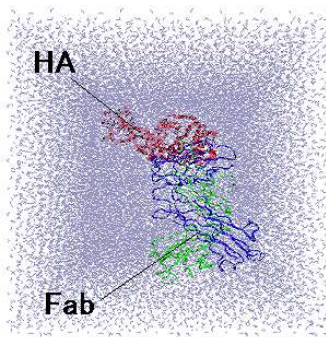


**FIGURE 2.** Solvated state of wild type HA and Fab fragment complex.

**TABLE 1.** MD condition.

Force Field Parameter:	Amber03
Ensemble:	NPT
Periodic boundary condition:	on
Cut off radius:	10.0Å
Shake:	Off(2VIR) , On(2VIS)
Time step:	1fs(2VIR) , 2fs(2VIS)
Solvate Water Box:	TIP3P(92.911,121.055,118.649 Å)

calculation. System minimization by steepest decent method of 2000 steps followed by conjugate gradient method of 18000 steps under constraint 30kcal/mol are executed for 25ps molecular dynamics simulation. Then, we released the constraint every 5kcal/mol over 25ps MD. We made the systems warm by heating MD from 100K to 300K every 5K over 10ps MD, and totally execute 200ps MD. Equilibrium of 800ps MD are followed. Detailed MD Conditions are shown in Table 1. After that, we estimated B-factor, binding free energy, and distance between atoms which contribute to hydrogen bonding.

## Theory

B-factor ( $B$ ) expresses fluctuation of compared to mean atomic position during total MD, which is defined by eqn.(1).

$$B = \frac{8}{3N} \pi^2 \sum_i^N \langle |R_i - \langle R_i \rangle|^2 \rangle \quad (1)$$

where  $N$  is the number of atom,  $R_i$  is coordinate of  $i$ -th atom, and  $\langle R_i \rangle$  is the ensemble average of  $R_i$ . Binding free energy between HA and Fab fragment is expressed by eqn.(2)-(4).[5][8]

$$\Delta G_{binding} = \langle G_{complex(i)} \rangle_i - \langle G_{Fab(i)} \rangle_i - \langle G_{HA(i)} \rangle_i \quad (2)$$

where  $\langle G_{complex(i)} \rangle_i$  is free energy of HA and Fab complex,  $\langle G_{Fab(i)} \rangle_i$  and  $\langle G_{HA(i)} \rangle_i$  are free energy of un-

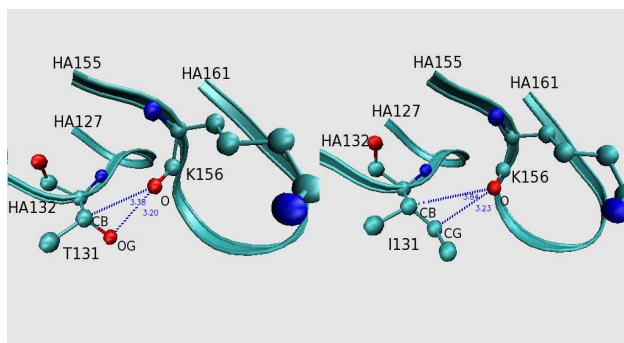


**FIGURE 3.** Distance between K156 carboxyl oxygen and T131 atoms in HA.(a):wild type HA(2VIR), (b):mutated HA(2VIS).

binded state of Fab and HA, respectively.  $i$  is the number of snapshot extracted from coordinates during MD.

$$G(i) = \langle E_{mm} \rangle_i + G_{solv}(i) - TS(i) \quad (3)$$

$$\langle E_{mm} \rangle = \langle E_{bond} \rangle + \langle E_{angle} \rangle + \langle E_{tors} \rangle + \langle E_{vdw} \rangle + \langle E_{elec} \rangle \quad (4)$$

where  $\langle E_{mm} \rangle$  is total internal molecular-mechanical energy, each terms correspond to the bond, angle, torsion, van der waals, and electrostatic term in molecular mechanical force field[13]. Total solvation energy  $G_{solv}$  of eqn.(3) is numerically calculated by the Poisson-Boltzmann equation, and estimates the nonpolar free energy with a simple surface area term[14, 15, 16].  $TS$  of eqn.(3) is the entropic contribution of solute, which can be estimated by normal-mode analysis[13].

## RESULTS AND DISCUSSION

### RMSD

We estimated RMSD of total residue and their loop structures in two different system by ptraj modules in AMBER 8. Compared to all residue, we found loop structures are relatively stable within extent from 0.5 to 1.6 angstrom (2VIR), and from 0.6 to 1.8 angstrom(2VIS). This RMSD difference between total residues and limited residues(loop structure) indicates that residues in the loop structures could easily reach equilibrium state. We also found RMSD value of 2VIR is smaller than that of 2VIS as a whole, it suggests that mutation caused structural change and energetic less favorable states that contributes to large deviation during total MD.

### B-factor

We calculated root mean square fluctuations (RMSF) and B-factor by ptraj. As shown in Table 2, the results

**TABLE 2.** B-factor average during 750-800ps MD.

	2VIR( $\text{\AA}^2$ )	2VIS( $\text{\AA}^2$ )	$\Delta$ ( $\text{\AA}^2$ )
HA127-132 residues	8.875	15.321	6.445
HA155-161 residues	11.544	13.820	2.276
HV1	8.785	16.741	7.956
HV2	12.864	24.315	11.451
HV3	12.740	15.959	3.219
LV1	16.413	17.829	1.416
LV2	19.497	22.211	2.714
LV3	18.187	17.249	-0.937

of 2VIR are smaller than those of 2VIS except for LV3. This qualitative tendency is also seen in RMSD result. In particular, B-factor difference( $\Delta$ ) of HA127-132, HV1, and HV2 are larger than other loop structures. These results indicates that mutation makes HA127-132 loop unstable and cause the less binding affinity to proximal HV1, HV2 loop structure.

### Binding Free Energy

Binding free energy in crystal atomic coordinates was calculated by MM-PBSA module. The results of the binding energy are summerised in Table 3. The relative tendency of binding energy and disassociation constant between 2VIR and 2VIS, is qualitatively similar. Above all results indicate that the more RMSD and B-factor increase, the less binding force the complex has.

### Loop structures in HA

According to the experiment[9], carboxyl oxygen in 156th lysine (K156@O) of the HA and side chain hydroxyl oxygen in 131th threonine (T131@OG) of the HA have much contribution to hydrogen bonding and complex's binding energy(Fig. 3). We estimated the four distances between the atoms, i.e, K156@O to  $\beta$ -

**TABLE 3.** Calculated Binding energy and Disassociation Constant derived from experiment.

	2VIR( $\text{\AA}^2$ )	2VIS( $\text{\AA}^2$ )	$\Delta$ (kcal/mol)
Binding Energy (kcal/mol)	32.2	46.52	14.32
Kd (exp.)[1]	$1.0 \times 10^{-9}$	$4.0 \times 10^{-6}$	
Kon (exp.)[1]	$1.1 \times 10^5$	$5.4 \times 10^2$	

**TABLE 4.** Average and standard deviation of the distance between HA K156 carboxyl oxygen and 131 amino acid atoms.

	2VIR( $\text{\AA}$ )	2VIS( $\text{\AA}$ )
K156@O and 131@CB(2VIR,2VIS)	$3.625 \pm 0.244$	$4.483 \pm 0.252$
K156@O and 131@OG(2VIR),CG(2VIS)	$2.857 \pm 0.225$	$3.509 \pm 0.202$

carbon (T131@CB) and K156@O to hydroxyl oxygen (T131@OG) in T131 of 2VIR, K156@O to  $\beta$ -carbon (I131@CB) and K156@O to  $\gamma$ -carbon (I131@CG) in I131 of 2VIS. The latter two atoms, I131@CB and I131@CG of the 2VIS, are located in almost same position as T131@CB and T131@OG of the 2VIR. The average and standard deviation of the distances are shown in Table 4. During total MD simulation, both atomic distances of 2VIR(K156@O to T131@CB and K156@O to T131@OG) are smaller than those of 2VIS(K156@O to I131@CB and K156@O to I131@CG). This results shows that K156@O and T131@OG in 2VIR are closed together, and they are easy to make hydrogen bonding. The hydrogen bond between K156@O and T131@OG is maintained even in solvent water surroundings, so that 2VIR's HA loop structure in binding site has a high structural stability, the binding affinity is maintained.

## CONCLUSION

We calculated Influenza Hemagglutinin and Fab fragment complex in water solvate surrounding. Calculation result of RMSD, B-factor and binding free energy suggests that wild type HA has much structural stability, which contributes to binding affinity with Fab fragment, especially in loop structures HA127-132, HV1, and HV2. To the contrary, mutated HA has much fluctuation in the three loop structures, that resulted in less structural stability. The reason for the difference of stability is the hydrogen bonding between K156@O and T131@OG in HA, which is maintained even in solvate states.

## ACKNOWLEDGMENTS

H.N. is grateful for financial support from the Ministry of Education, Science and Culture of Japan(grant

15550010).

## REFERENCES

1. D. R. Davies, and S. Chacko, *Acc. Chem. Res.* **26**, 421–427 (1993).
2. C. A. Sotriffer, W. Flader, R. H. Winger, B. M. Rode, K. R. Liedl, and J. M. Varga, *Methods* **20**, 280–291 (2000).
3. J. Aqvist, C. Medina, and J. E. Samuelsson, *Protein Engineering* **7**, 385–391 (1994).
4. B. Jayaram, D. Sprous, M. A. Young, and D. L. Beveridge, *J. Am. Chem. Soc.* **120**, 10629–10633 (1998).
5. P. A. Kollman, I. Massova, C. Reyes, B. Kuhn, S. Huo, L. Chong, M. Lee, T. Lee, Y. Duan, W. Wang, O. Donini, P. Cieplak, J. Srinivasan, D. A. Case, and T. E. Cheatham III, *Acc. Chem. Res.* **33**, 889–897 (2000).
6. L. T. Chong, Y. Duan, L. Wang, I. Massova, and P. A. Kollman, *PNAS* **96**, 14330–14335 (1999).
7. B. Kuhn, and P. Kollman, *J. Med. Chem.* **43**, 3786–3791 (2000).
8. H. Gohlke, and D. A. Case, *J. Comput. Chem* **2004**, 238–250 (2004).
9. D. Fleury, S. A. Wharton, J. J. Skehel, M. Knossow, and T. Bizebard, *Nature Structural Biology* **5**, 119–123 (1998).
10. T. Kinoshita, M. Hata, S. Neya, T. Hoshino, and C. Obinata, *Symposium on Chemical Information and Computer Sciences Tokyo*, JP12 (2003).
11. D. A. Pearlman, D. A. Case, J. W. Caldwell, T. E. Cheatham III, W. S. Ross, S. DeBolt, D. Ferguson, S. Geibel, and P. A. Kollman, *Comp. Phys. Commun.* **91**, 1–41 (1995).
12. W. L. Jorgensen, J. Chandrasekhar, J. Madura, R. Impey, and M. L. Klein, *J. Chem. Phys.* **79**, 926–935 (1983).
13. J. Srinivasan, T. E. Cheatham III, P. Cieplak, P. A. Kollman, and D. A. Case, *J. Am. Chem. Soc.* **120**, 9401–9409 (1998).
14. D. Sitkoff, *J. Phys. Chem.* **98**, 1978–1983 (1998).
15. J. M. J. Swanson, S. A. Adcock, and J. A. McCammon, *J. Chem. Theory Comput.* **1**, 484–493 (2005).
16. K. Sharp, J. A. Charles, and B. Honig, *J. Phys. Chem.* **96**, 3822–3828 (1992).